

Momentum distribution curves in the superconducting state

M. R. Norman,¹ M. Eschrig,¹ A. Kaminski,² and J. C. Campuzano^{1,2}

¹Materials Science Division, Argonne National Laboratory, Argonne, Illinois 60439

²Department of Physics, University of Illinois at Chicago, Chicago, Illinois 60607

(Received 29 May 2001; published 18 October 2001)

We demonstrate that the E vs \mathbf{k} dispersion in the superconducting state extracted from momentum-distribution curves differs qualitatively from the traditional dispersion extracted from energy-distribution curves. This occurs because of a combination of many-body effects and the presence of an energy gap, along with the associated coherence factors. Analysis of such momentum-distribution-curve dispersions can give important information on the microscopics of high-temperature superconductors.

DOI: 10.1103/PhysRevB.64.184508

PACS number(s): 74.72.Hs, 74.25.Jb, 79.60.Bm

Traditionally, practitioners in angle-resolved photoemission spectroscopy (ARPES) have analyzed data at fixed momentum as a function of binding energy, so-called energy distribution curves (EDC's). Recent advances in analyzer technology have allowed the probing of electronic states via ARPES to a much higher precision in momentum space than previously attainable.¹ This has led to the realization that additional information can be obtained by analyzing data at fixed binding energy as a function of momentum, so-called momentum distribution curves (MDC's). Such MDC's have been used in high-temperature cuprate superconductors for a variety of purposes, including the testing of the marginal Fermi-liquid hypothesis,^{2,3} and the elucidation of a dispersion kink along the nodal direction,⁴ the origin of which is currently being debated.⁵⁻⁷

Analysis of MDC's in the normal state, or in the superconducting state along the nodal direction, is relatively straightforward because of the absence of an energy gap.⁵ As we demonstrate in this paper, qualitative changes occur in the MDC's due to the energy gap. By analyzing MDC dispersions, one can gain important information on many-body effects in the superconducting state.

The data reported in this paper were obtained at the Synchrotron Radiation Center, Wisconsin, using a Scienta SES 200 analyzer, and were previously used in earlier work.⁵ A photon energy of 22 eV was employed with the optimal doped ($T_c = 90$ K) $\text{Bi}_2\text{Sr}_2\text{CaCu}_2\text{O}_{8+\delta}$ (Bi2212) sample in a Γ - M polarization geometry. The chemical potential was determined from a polycrystalline Au sample in electrical contact with the Bi2212 sample.

As previously reported,⁵ we have taken data for a number of momentum-cuts in the Brillouin zone both in the normal and superconducting states. In this paper, we will concentrate our attention on a particular momentum-cut intermediate between the (π, π) direction, where the superconducting gap vanishes, and the $(\pi, 0)$ region, where the superconducting gap is maximal. The reason for avoiding $(\pi, 0)$ is that a combination of matrix-element effects, superstructure images, and the pseudogap complicate the interpretation of MDC's in this region of the zone⁸ (for the chosen cut, these complications are not present). MDC and EDC dispersions were obtained from the maxima of the respective curves.

In Fig. 1(a), MDC dispersions are shown in both the normal and superconducting states. The normal state dispersion

is roughly linear in \mathbf{k} in the energy range of interest. In the range of 20–60 meV, the superconducting dispersion is also linear, but with a slope approximately half that of the normal state, as noted earlier.³ This implies an additional many-body renormalization of the superconducting-state dispersion relative to that in the normal state. Another effect of this renormalization can be seen at binding energies higher than 60 meV, where the dispersion goes almost vertical before recovering back to the normal-state dispersion.

To understand this effect in greater detail, we compare in Fig. 1(b) the dispersions in the superconducting state obtained from MDC's and EDC's. As noted in an earlier paper,⁵ the EDC dispersions contain two branches, a lower-binding-energy “quasiparticle” branch, and a higher-binding-energy branch [known as the “hump” in the $(\pi, 0)$ region]. We see, then, that the vertical part of the MDC dispersion corresponds to a crossover between the low-energy and high-energy EDC branches. These effects are typical of electrons interacting with a bosonic mode,^{9,10} and the mode in the current case has been identified as a spin exciton by some authors^{11,5,7} and a phonon by others.⁶ As can be seen from Fig. 1(b) and also noted above [Fig. 1(a)], the renormalization is an *additional* effect associated with the superconducting state, and thus unlikely to be due to a phonon.

Moreover, in Fig. 2, we show the MDC and EDC disper-

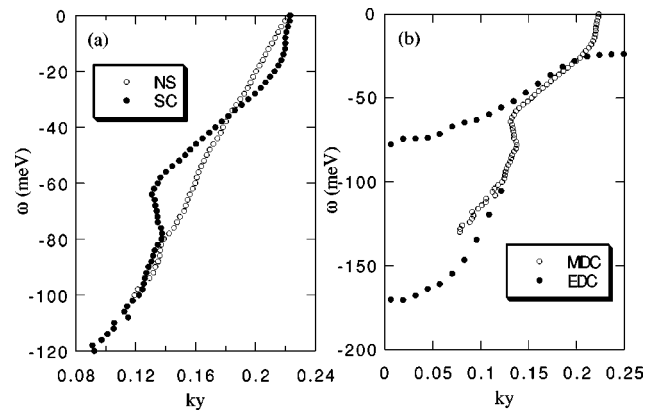


FIG. 1. (a) MDC dispersion in the superconducting state (SC, $T=40$ K) versus that in the normal state (NS, $T=140$ K). (b) MDC versus EDC dispersion in the superconducting state. k_y is in units of π/a . For this momentum cut, $k_x = 0.59\pi/a$.

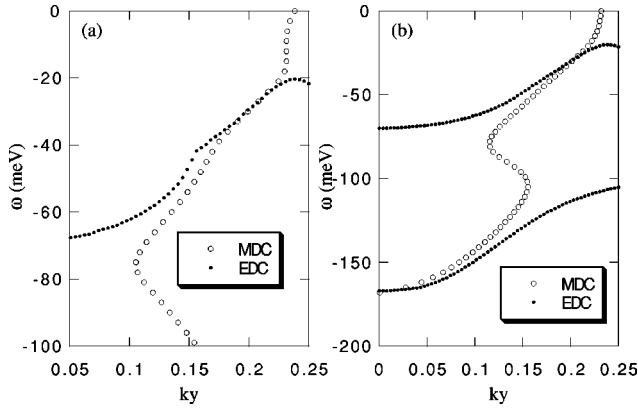


FIG. 2. MDC and EDC dispersions in the superconducting state from the spin-exciton model of Ref. 12 ($\Gamma = 10$ meV, mode energy $\Omega = 39$ meV, coupling constant $g = 0.65$ eV, maximum gap $\Delta_0 = 46$ meV). The energy resolution is $\sigma = 1$ meV in (a) and 7 meV in (b). In (a), the weak kink in the EDC quasiparticle branch marks the mode energy, which is washed out in (b) due to resolution. The higher-energy structure associated with the S shape in the MDC dispersion is due to the strong frequency dependence of the self-energy around $\Delta_0 + \Omega$.

sions calculated from the spin exciton model.¹² This model describes the interaction of the electrons with the sharp magnetic resonance seen in the superconducting state by inelastic neutron scattering. We see that this calculation gives a good description of the experimental data of Fig. 1(b), and demonstrates the pronounced effect of momentum-dependent many-body interactions on the shape of the MDC and EDC dispersions. This calculation also reproduces the difference between the MDC and EDC dispersions in the “linear” regime (20–60 meV), which as we demonstrate below, does not occur in a BCS model. The difference in the spin-exciton case is associated with the nontrivial frequency dependence of the electron self-energy, which occurs because of the presence of a sharp energy scale associated with the magnetic resonance. That is, the two dispersions differ since the MDC probes the self-energy as a function of momentum at fixed frequency, whereas the EDC probes the self-energy as a function of frequency at fixed momentum.

For the remainder of the paper, we concentrate on the low-binding-energy range, where the data are characterized by a renormalized “quasiparticle” branch, and a simpler analysis of the data is possible. Returning to Fig. 1(a), we note that for binding energies lower than 20 meV, the MDC dispersion in the superconducting state goes almost vertical, and at zero energy it is close to the normal-state Fermi momentum. By looking at Fig. 1(b), where the MDC and EDC dispersions are compared, we notice that the upturn in the MDC dispersion corresponds to entering the subgap region identified from the EDC dispersion.

Unfortunately, a model-independent analysis of the data is somewhat impractical, as noted in passing in an earlier paper.⁵ This can be easily seen by a quick look at the BCS theory. In this theory, the effect of superconductivity can be represented by a self energy of the form $\Delta_{\mathbf{k}}^2/(\omega + \epsilon_{\mathbf{k}} + i0^+)$, where $\Delta_{\mathbf{k}}$ is the superconducting energy gap and $\epsilon_{\mathbf{k}}$ is the normal-state dispersion. Note that this self-energy has a non-

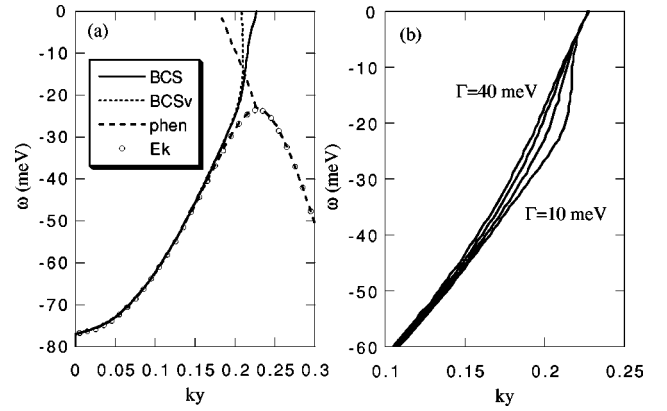


FIG. 3. Theoretical MDC dispersion in the superconducting state. (a) Curves correspond to Eq. (2) (BCS), second term in Eq. (2) only (BCSv), and Eq. (3) (phen). The circles are the BCS-energy dispersion, $\omega = -E_{\mathbf{k}}$. The parameters are listed in the text ($\Gamma = 15$ meV). (b) Results from Eq. (2) as a function of the broadening parameter Γ .

trivial dependence on momentum (that is, it is not linear in \mathbf{k}), and thus invalidates a simple Lorentzian analysis of the MDC’s. This behavior is characteristic of any system that contains an energy gap.

We have thus looked at a simple model to describe the MDC superconducting dispersion in the low-energy range. Simple BCS theory will not work, since by definition it has no solution in the subgap energy range (the spectral function in this case is just a δ function). The simplest generalization is to use a self-energy of the form¹³

$$\Sigma = -i\Gamma_1 + \Delta_{\mathbf{k}}^2/(\omega + \epsilon_{\mathbf{k}} + i\Gamma_0). \quad (1)$$

The case where $\Gamma_1 = \Gamma_0 = \Gamma$ is just a broadened version of the BCS theory¹⁴ and we find that it gives a good account of the data.

For $\Delta_{\mathbf{k}}$, we assume a *d*-wave energy gap of the form $\Delta_0[\cos(k_x a) - \cos(k_y a)]/2$ where Δ_0 is fit by the energy of the quasiparticle peak in the EDC at the Fermi momentum. We find that $\epsilon_{\mathbf{k}}$ is consistent with our earlier tight-binding fit to normal-state data¹⁵ if a scaling factor z is introduced to account for the additional many-body renormalization of the superconducting-state dispersion relative to the normal-state dispersion discussed above in the context of Fig. 1 (for the momentum cut considered here, $z = 0.61$). The EDC peak energy, 24 meV, sets Δ_0 to be 46 meV. At this stage, we will assume that all the broadening is due to Γ , which is obtained by fitting the top of the EDC peak at the Fermi momentum (giving 15 meV). The effect of energy and momentum resolution broadening will be treated later.

In Fig. 3(a), we show our theoretical MDC dispersion and compare it to some alternate theoretical curves to be discussed below. To appreciate these results, we remind the reader that the broadened BCS spectral function can be written as^{14,16}

$$\pi A(\mathbf{k}, \omega) = \frac{u_{\mathbf{k}}^2 \Gamma}{\Gamma^2 + (\omega - E_{\mathbf{k}})^2} + \frac{v_{\mathbf{k}}^2 \Gamma}{\Gamma^2 + (\omega + E_{\mathbf{k}})^2} \quad (2)$$

where $u_{\mathbf{k}}$ and $v_{\mathbf{k}}$ are the BCS coherence factors, and $E_{\mathbf{k}} = \sqrt{\epsilon_{\mathbf{k}}^2 + \Delta_{\mathbf{k}}^2}$ are the BCS-quasiparticle energies. The simplest MDC is for $\omega=0$. In this case, the right-hand side simply reduces to $\Gamma/(\Gamma^2 + E_{\mathbf{k}}^2)$. Ignoring the weak variation of $\Delta_{\mathbf{k}}$ with \mathbf{k} , one has a peak centered at $\epsilon_{\mathbf{k}}=0$, i.e., at the Fermi momentum $\mathbf{k}_{\mathbf{F}}$. An important point is that for this case, the coherence factors drop out, and it is for this reason that the peak is at $\mathbf{k}_{\mathbf{F}}$.

Now consider $\omega < 0$ (occupied states), but within the sub-gap region. If it were not for the coherence factors, the MDC peak would still be centered at $\mathbf{k}_{\mathbf{F}}$, i.e., the dispersion would be vertical. But, the coherence factors skew the peak to be centered at $\mathbf{k} < \mathbf{k}_{\mathbf{F}}$. This trend becomes more pronounced as Γ increases as can be seen in Fig. 3(b), where the MDC dispersion increasingly resembles the normal state.

As an exercise, we show the MDC dispersion in Fig. 3(a), but where only the second term in Eq. (2) is included. This corresponds to ignoring the influence of the unoccupied ($\omega > 0$) dispersion branch on the occupied MDC's ($\omega < 0$). In this case, the MDC dispersion becomes vertical in the sub-gap region, but with an $\omega=0$ value significantly displaced from $\mathbf{k}_{\mathbf{F}}$, the displacement being due to the skewing caused by the \mathbf{k} dependence of $v_{\mathbf{k}}$. Physically, this behavior could occur if the Γ value for the first term in Eq. (2) was significantly smaller than that for the second term (in which case the first term would not influence the MDC's for $\omega < 0$). We note that several microscopic theories for the cuprates do in fact predict this behavior.¹⁷ That is, the broadening is significantly reduced for unoccupied states as compared to occupied ones. Therefore, we see from the difference in the sub-gap dispersions in these two cases that the MDC dispersion is not only a sensitive test of the coherence factors, but also the particle-hole symmetry of the self-energy as well, even when looking at just the occupied states. Moreover, as we discuss below, energy resolution will cause this skewing of the dispersion to occur as well.

Another curve is shown in Fig. 3(a), and that is where Γ_0 [Eq. (1)] is set to 0. This self-energy is essentially the one used in our earlier work¹³ in the superconducting state, and corresponds to having no broadening in the BCS (pairing) part of the self-energy. Although this model gives a good description of the low-energy part of the EDC at $\mathbf{k}_{\mathbf{F}}$, it gives an erroneous MDC dispersion. This can be understood from the spectral function of this model,

$$\pi A(\mathbf{k}, \omega) = \frac{\Gamma}{\Gamma^2 + (\omega + E_{\mathbf{k}})^2 [(\omega - E_{\mathbf{k}})/(\omega + \epsilon_{\mathbf{k}})]^2}. \quad (3)$$

It has been factored in such a way so as to emphasize the $\omega < 0$ branch. Note that this is not of the form of Eq. (2). In particular, the term in brackets in the denominator of Eq. (3) plays the same role that the coherence factors do in Eq. (2), but in this case this factor is ω dependent. At $\omega=0$, the MDC is zero at $\mathbf{k}_{\mathbf{F}}$, that is, the MDC has a minimum rather than a maximum as in Eq. (2). Because of this, the MDC dispersion has a very strange behavior in the sub-gap region. Moreover, for $\omega < -\Delta$, the MDC dispersion becomes similar to the EDC dispersion, reflecting the dispersion of $E_{\mathbf{k}}$. This

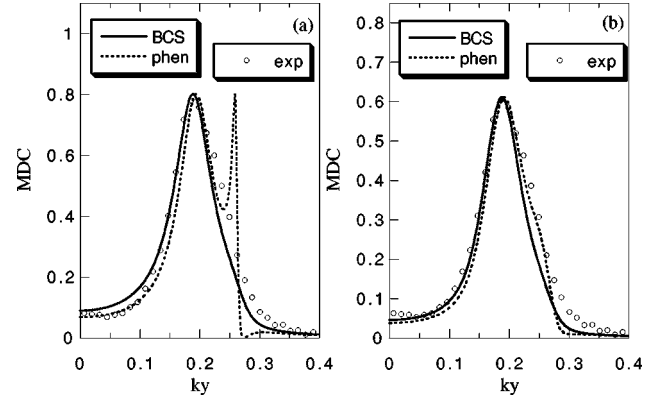


FIG. 4. (a) Theoretical MDC in the superconducting state from Eq. (2) (BCS) and Eq. (3) (phen), compared to experiment (open circles). $\omega = -30$ meV and $\Gamma = 15$ meV. (b) Same results, but including energy resolution ($\sigma = 7$ meV, $\Gamma = 10$ meV).

is because of the peculiar “coherence” factors, which lead to a sharp second peak in the MDC for $\mathbf{k} > \mathbf{k}_{\mathbf{F}}$ corresponding to the particle-hole image of the dispersion for positive ω , as shown in Fig. 4(a) [the sharpness is due to the removal of broadening in the pairing part of the self-energy in Eq. (1)]. This subsidiary peak is strongly reduced in Eq. (2) (consistent with experiment), as can also be seen in Fig. 4(a). To test this further, we have done two-dimensional ω - \mathbf{k} intensity plots, and find that Eq. (2) gives an intensity profile similar to experiment. This is in contrast with results obtained from Eq. (3), reminiscent of pure BCS theory (i.e., zero broadening), where a pronounced intensity is seen for $\mathbf{k} > \mathbf{k}_{\mathbf{F}}$, reflecting the “backbending” expected from the $E_{\mathbf{k}}$ dispersion. This is not seen in experiment, and reiterates our point that the MDC's and intensity profiles are quite sensitive to self-energy effects and coherence factors.

We now discuss the effects of momentum and energy resolution. We have verified by calculation that the small momentum window of the Scienta analyzer (a rectangle of dimensions $0.01\pi/a$ along the cut and $0.02\pi/a$ transverse to the cut) has no effect on the results. This is not true for the energy resolution. The latter can be determined by fitting the leading edge of the Au spectrum, which for the present data gives a Gaussian σ of 7 meV [full width at half maximum (FWHM) of 16–17 meV]. As an initial exercise, let us assume that all the broadening is due to energy resolution (for 30 meV FWHM, this would yield a σ of 12.8 meV). Then, in the BCS case with the spectral function as δ functions, the MDC's are very easy to determine. For an energy gap much larger than temperature (satisfied here, since the EDC peak energy at the Fermi momentum is 24 meV and the temperature is 40 K), the $u_{\mathbf{k}}$ term drops out [$f(E_{\mathbf{k}})$ is essentially zero]. Doing the energy-resolution convolution, the ARPES intensity is simply $v_{\mathbf{k}}^2 \exp[-(\omega + E_{\mathbf{k}})^2/2\sigma^2]$. Since the intensity is totally controlled by the $v_{\mathbf{k}}$ term, the MDC dispersion will obviously be skewed, as demonstrated in Fig. 5(a), where this result is compared to the previous broadened BCS case of Fig. 3(a). In particular, the MDC dispersion at zero energy yields a momentum value, which is slightly displaced

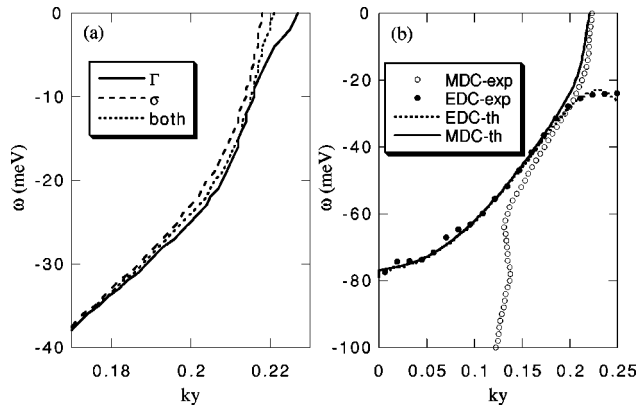


FIG. 5. (a) The effect of energy resolution on the MDC dispersion from Eq. (2). The curves correspond to $\Gamma=15$ meV, $\sigma=0$ (Γ), $\Gamma=0$, $\sigma=12.8$ meV (σ), and $\Gamma=10$ meV, $\sigma=7$ meV (both). (b) Comparison of theoretical (th) and experimental (exp) MDC and EDC dispersions. For theory, $\Gamma=10$ meV, $\sigma=7$ meV.

from the normal-state Fermi momentum, and the MDC dispersion in the subgap region is more vertical than in the Γ -broadened case.

Also shown in Fig. 5(a) is the more realistic case where both effects are incorporated. Given the actual experimental σ of 7 meV, a Γ of 10 meV is necessary to reproduce the 30 meV FWHM of the EDC peak. As expected, the combined result is intermediate between the two limiting cases. Moreover, the inclusion of energy resolution lessens the difference between the MDC profiles of the two self-energy models presented in Fig. 4(a), as illustrated in Fig. 4(b). An advantage of the model of Eq. (3) is that it can account for the

extra experimental weight on the trailing (unoccupied) edge of the MDC peak (due to the particle-hole image), which is not present in the broadened BCS model. In fact, by looking at experimental MDC's at higher binding energies, a weak shoulder does develop on the trailing edge, corresponding to the expected particle-hole image discussed earlier. This image should become better defined with improved resolution and statistics.

In fact, it is somewhat remarkable that the simple form of Eq. (2) does such a good job in describing the data. In Fig. 5(b), we compare the MDC and EDC dispersions of Fig. 1(b) to our calculation of Fig. 5(a). Confining ourselves to the “quasiparticle” branch, the agreement of experiment and theory is quite good. But, the discrepancy between the MDC and EDC dispersions in the “linear” regime (20–60 meV) is not reproduced by the BCS theory, though it can be accounted for in the spin-exciton model as demonstrated in Fig. 2 due to the nontrivial frequency dependence of the self-energy in that model.

In conclusion, we find that the MDC's and resulting dispersions are nontrivial in the superconducting state, and give important information on the electron self-energy and coherence factors. We feel that a more detailed study of MDC's, both in the superconducting and pseudogap phases, will give important insights into the microscopics of high-temperature cuprate superconductors. We hope to report on such studies in a future paper.

This work was supported by the U.S. Department of Energy, Office of Science, under Contract No. W-31-109-ENG-38 and the National Science Foundation Grant No. DMR 9974401.

- ¹A. Kaminski, J. Mesot, H. Fretwell, J. C. Campuzano, M. R. Norman, M. Randeria, H. Ding, T. Sato, T. Takahashi, T. Mochiku, K. Kadowaki, and H. Hoehst, *Phys. Rev. Lett.* **84**, 1788 (2000).
- ²T. Valla, A. V. Fedorov, P. D. Johnson, B. O. Wells, S. L. Hulbert, Q. Li, G. D. Gu, and N. Koshizuka, *Science* **285**, 2110 (1999).
- ³T. Valla, A. V. Fedorov, P. D. Johnson, Q. Li, G. D. Gu, and N. Koshizuka, *Phys. Rev. Lett.* **85**, 828 (2000).
- ⁴P. V. Bogdanov, A. Lanzara, S. A. Kellar, X. J. Zhou, E. D. Lu, W. Zheng, G. Gu, J.-I. Shimoyama, K. Kishio, H. Ikeda, Z. Hussain, R. Yoshizaki, and Z. X. Shen, *Phys. Rev. Lett.* **85**, 2581 (2000).
- ⁵A. Kaminski, M. Randeria, J. C. Campuzano, M. R. Norman, H. Fretwell, J. Mesot, T. Sato, T. Takahashi, and K. Kadowaki, *Phys. Rev. Lett.* **86**, 1070 (2001).
- ⁶A. Lanzara, P. V. Bogdanov, X. J. Zhou, S. A. Kellar, D. L. Feng, E. D. Lu, T. Yoshida, H. Eisaki, A. Fujimori, K. Kishio, J.-I. Shimoyama, T. Noda, S. Uchida, Z. Hussain, and Z.-X. Shen, *Nature (London)* **412**, 510 (2001).
- ⁷P. D. Johnson, T. Valla, A. V. Fedorov, Z. Yusof, B. O. Wells, Q. Li, A. R. Moodenbaugh, G. D. Gu, N. Koshizuka, C. Kendziora, S. Jian, and D. G. Hinks, cond-mat/0102260, *Phys. Rev. Lett.* (to be published).

- ⁸H. M. Fretwell, A. Kaminski, J. Mesot, J. C. Campuzano, M. R. Norman, M. Randeria, T. Sato, R. Gatt, T. Takahashi, and K. Kadowaki, *Phys. Rev. Lett.* **84**, 4449 (2000).
- ⁹D. J. Scalapino, in *Superconductivity*, edited by R. D. Parks (Dekker, New York, 1969), Vol. 1, p. 449.
- ¹⁰M. R. Norman and H. Ding, *Phys. Rev. B* **57**, R11 089 (1998).
- ¹¹M. R. Norman, H. Ding, J. C. Campuzano, T. Takeuchi, M. Randeria, T. Yokoya, T. Takahashi, T. Mochiku, and K. Kadowaki, *Phys. Rev. Lett.* **79**, 3506 (1997).
- ¹²M. Eschrig and M. R. Norman, *Phys. Rev. Lett.* **85**, 3261 (2000).
- ¹³M. R. Norman, M. Randeria, H. Ding, and J. C. Campuzano, *Phys. Rev. B* **57**, R11 093 (1998).
- ¹⁴J. R. Schrieffer, *Theory of Superconductivity* (Benjamin, New York, 1964).
- ¹⁵M. R. Norman, M. Randeria, H. Ding, and J. C. Campuzano, *Phys. Rev. B* **52**, 615 (1995).
- ¹⁶J. C. Campuzano, H. Ding, M. R. Norman, M. Randeria, A. F. Bellman, T. Yokoya, T. Takahashi, H. Katayama-Yoshida, T. Mochiku, and K. Kadowaki, *Phys. Rev. B* **53**, R14 737 (1996).
- ¹⁷P. A. Lee and N. Nagaosa, *Phys. Rev. B* **46**, 5621 (1992); B. Janko, J. Maly, and K. Levin, *ibid.* **56**, R11 407 (1997).